Polymer Bulletin 47, 587-594 (2002)

Polymer Bulletin

Glass bead filled polystyrene composites: morphology and fracture

M. Sánchez-Soto (✉) , A. Gordillo, M. LL. Maspoch, J.I. Velasco, O.O Santana, A.B. Martínez

Centre Català del Plàstic, Dpt. Ciència dels Materials i Enginyería Metal.lúrgica, Universitat Politècnica de Catalunya (UPC), C/Colom 114, 08222 Terrassa

Received: 17 July 2001/Revised version: 18 December 2001/ Accepted: 12 January 2002

Summary

The objectives of this work are to describe the fracture behaviour of a material model composed by polystyrene and different amounts of solid glass beads. Seven compositions with beads content ranging between 0 % and 40 % by weight, have been prepared. A morphology study has been carried out to examine the microstructure developed during injection moulding. Fracture parameters (K_{IC}, G_{IC} and J_{IC}) were calculated at high and low strain rate as a function of particle content. The maximum reinforcement was found at middle levels of glass beads (6%-15%wt). The composite fracture behaviour at low strain rate was always brittle although it was found that beads tend to stabilize its propagation. At high strain rate, the particle reinforcement effect is lower, however a small increment in K_{IC} and G_{IC} was found.

Introduction

A large amount of thermoplastics are available with fillers that are added mainly to increase material stiffness. However, the incorporation of fillers into thermoplastics modifies several properties. The knowledge of some of these changes is necessary in order to improve the final composite behaviour.

Polystyrene (PS) is an amorphous glassy thermoplastic where crazing is the dominant deformation mechanism [1-2]. Glass beads are preferred as fillers especially when composite properties such as isotropy or low melt viscosity are important. Moreover, the orientation effects associated to moulding are minimal. As a result, polystyrene-glass beads system would be, in advance, an uniformly reinforced system.

Linear elastic fracture mechanics (LEFM) has been widely employed to study the fracture toughness of glassy thermoplastics [3,4]. When LEFM requirements can not be satisfied, toughness characterization based on the elastic-plastic fracture mechanics (EPFM) can be used. To determine the fracture toughness value (J_C) the procedures proposed by ESIS [4], Narisawa [5] and master curve [6] have been compared. It is well known that morphology could influence the sample mechanical response. In addition, morphology is also dependent of the flow behaviour developed during processing and this could be altered by the filler [7]. Thus, a morphological analysis has been carried out to determine the obtained particle dispersion.

Materials and composition

A commercial polystyrene (Lacqrene 1541) supplied by Elf-Atochem was employed as matrix. This is a high fluidity grade (melt flow index=12 gr/10 min. at 5 Kg and 200°C) and contains 5% wt. of mineral oils. The presence of mineral oils or lubricant is desirable to obtain consistent fracture parameters [1],[8-9]. Glass beads with an average particle size of 27.4 μm. and size distribution range between 2 μm. and 120 μm., were supplied by Sovitec Ibérica S.A.
The compounding process was carried out using a Collin co-rotating twin-screw extruder with length to diameter ratio of 24. Seven different compositions were obtained with beads content ranging from 0 to 40 % wt, (table 1). Once obtained, the extruded was feed into an injection-moulding machine with 90 Tons of clamping force. Prismatic specimens were moulded according to ASTM D-647 [10]. Temperature profile from hopper to die was 185-210-215-225-235-240°C. Samples were finally tempered at 70°C for 6 hours.

Experimental details

Particle content and morphological analysis

Ash method was used to determine particle concentration. Specimens were extracted from the center of the prismatic bars that were selected randomly. The filler volume fraction was obtained through density measurement. Results are shown in table 1
To take into account the particle distribution, firstly, a weight filler analysis was practiced in the zones represented in figure 1. In this case ashing was carried out over the A40 composition, where differences are expected to be most significant. The analysis was performed along X (injection direction) and Y-axis, (transverse direction). Results are displayed in figure 2a and 2b respectively. In second term, the composite morphology was qualitatively analyzed by optical microscope observation. For this analysis, the cuts located at X2 = 0.25 L, X3 = 0.5 L, X4 = 0.7 L and X5 = 0.9 L where selected. Due to the injection point closeness, the section at X1 = 0.05 L was not considered. Prior to observation each cut was carefully polished.

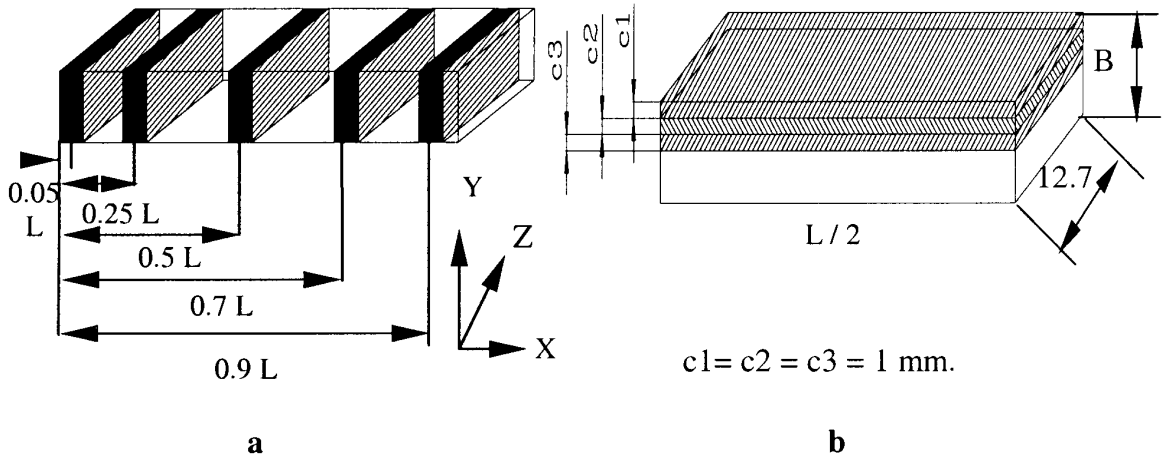

Figure 1. Schematic representation of the practiced cuts: a: X direction cuts. b: Y direction cuts. The injection point is located face centered in X= 0. L = 127 mm. B=6.35 mm.

Fracture test

Low strain velocity fracture tests were carried out in a mechanical testing machine setting the grids approach velocity to 1 mm/min. Multiple specimen technique was employed in LEFM and EPFM analysis. Single-edge notched three-point bend specimens (SENB) with dimensions of 12.7 x 6.35 x 63.5 mm^3 (width-thickness-length) were centrally notched on the narrow specimen side. Notches were further sharpened with a razor blade. Cracks of different lengths were inserted using this procedure. For LEFM the crack lengths vary between:

$$0.45 \leq a_0 / w \leq 0.55 \quad (1)$$

and for EPFM:

$$0.55 \leq a_0 / w \leq 0.65 \quad (2)$$

were a_0 is the pre-crack length, and w is the specimen width.
J-integral value was determined accordingly with the following equation [4,5]

$$J = \frac{2U^*}{B(w - a_0)}\left[1 - \frac{0.5\Delta a}{(w - a_0)}\right] \quad (3)$$

In the previous equation, U* is the energy determined from the area under the load-displacement curve once corrected for indentation effects, B is the sample thickness, w is the sample width, and a_0 is the pre-crack length. Δa is the difference between the final crack length and the initial pre-crack length.
High-rate fracture tests were performed over identical SENB specimens prepared as above. Specimens where placed on an instrumented Charpy pendulum equipped with a 2.5 Kg hammer. Impact velocity was set up to 0.5 m/s.

Results and discussion

Particle content and morphology

Glass beads content analysis, throws, for all samples, very close values to the initial nominal ones. Results are summarized in Table 1

Table 1. Nominal and experimental glass beads content

Sample id.	Nominal weight (%)	Calculated weight (%)	Filler volume fraction (ϕ)
PS	0	0	0
A2	2	1.91 ± 0.02	0.82± 0.02
A6	6	6.25 ± 0.17	2.77± 0.07
A10	10	10.16 ± 0.03	4.62± 0.01
A15	15	14.78 ± 0.14	6.91± 0.06
A25	25	25.38 ± 0.07	12.79± 0.03
A40	40	40.16 ± 0.51	22.36± 0.28

Figure 2 shows the glass beads concentration evolution over the prismatic bar from injection point to the bar end (a) and from center to edge (b) in A40 sample. Differences were small, however the total particle number tends to increase as we move far away from the injection point with a maximum located between 0.5L and

0.7L in the X direction, and between 4 and 5 mm in Y direction. This fact agree well with the observations of Ogadhoh [11], who found small deviations using glass beads sizes up to 150 μm.

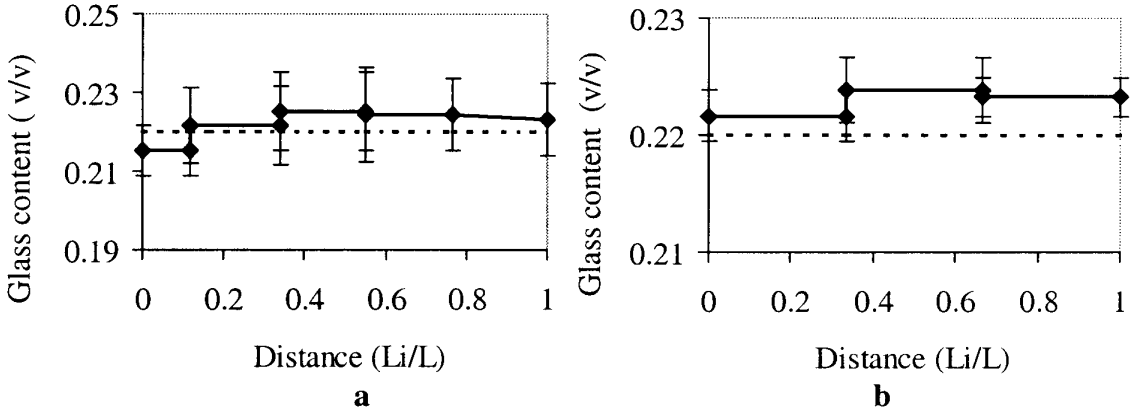

Figure 2. Glass bead content as a function of specimen length. A40 sample. Dotted line represents nominal glass bead content. a: X cuts. b: Y cuts. Li : cut position.

Microscopically observation of transversal sample sections shows a random particle distribution. In Figure 3 are depicted the photographs belonging to central cuts (X=0,5L) for two different compositions. It is important to notice the absence of particle aggregates, even in the most filled sample. Further, particle-depleted zones were neither found.

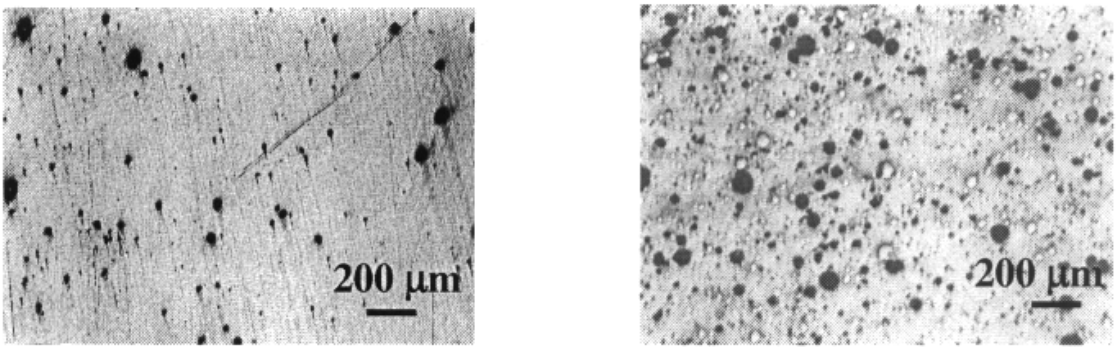

Figure 3. Particle distribution in central sample sections (X=0.5 L). Flow is perpendicular to the page. From left to right samples A2 and A40.

The good particle dispersion is a consequence of the efficiency of the twin-screw extruder coupled with the high flow matrix. Taken this into account it is possible to assess that particle dispersion will not affect the composite mechanical behavior.

Fracture behaviour

Low strain rate

The fracture of polystyrene-glass bead composites has shown different trends depending on the glass bead content. Polystyrene and A2 accomplish LEFM criteria and show unstable fracture. A6 composition has an intermediate behaviour with stable and unstable fracture propagation. Higher contents of glass beads (A10 ÷ A40) gave stable fracture and were studied by J-integral criterion. Table 2 reports the results.

Table 2. K_{IC}, G_{IC}, and J values for some polystyrene-glass bead samples.

Sample	K_{IC} (Mpa $m^{1/2}$)	r^2	G_{IC} (KJ/m^2)	r^2	$J_{0,2\text{-}E}$ (KJ/m^2)	$J_{0\text{-}N}$ (KJ/m^2)	$J_{C\text{-}P}$ (KJ/m^2)
PS	1.43	0.98	0.66	0.91			
A2	1.62	0.94	0.85	0.84			
A6	1.87	0.96	1.18	0.87			
A10					1.05	0.92	1.01
A15					1.21	1.00	1.15
A25					1.02	0.75	0.93
A40					0.87	0.69	0.73

Polystyrene fracture parameters are quite variable [1]. In our case, this variability is reduced by the presence of lubricants that allows a large elongation of craze fibrils. In this situation crack tends to propagate through the craze interior,

When there is a small quantity of non-bonded beads in the matrix, like in A2 sample, a few crazes are generated near the particle equator [12]. In this situation, the polystyrene unstable propagation still prevails, but the generation of a set of crazes at the crack tip increases K_{IC} and G_{IC}. As more particles are added to matrix, the generated crazes become small in size but large in number, due to the appearance of multiple stress points. Then, crack propagates through bunches of crazes increasing the size of plastic deformation zone and K_{IC}.

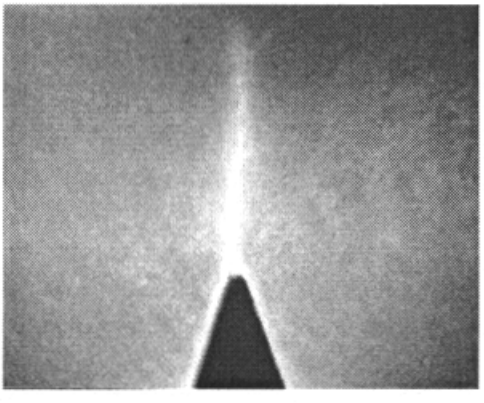

Figure 4. Crack tip propagation and plastic zone at A40 sample.

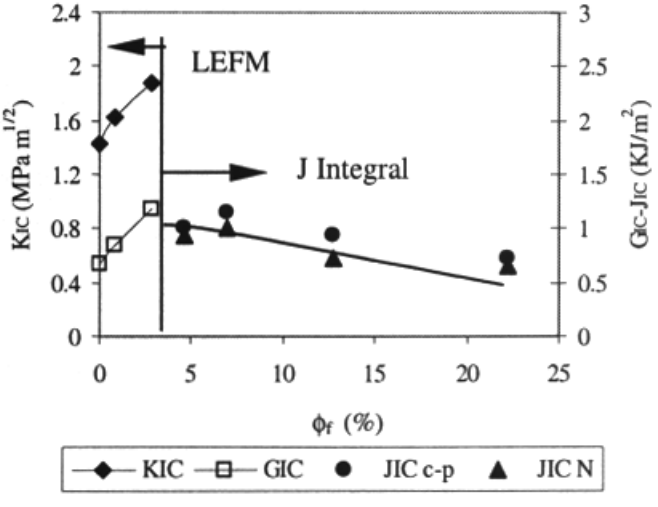

Figure 5. Evolution of K_{IC}, G_{IC} and J_{IC} vs. filler volume (%)

Elastic-plastic analysis has been applied to samples with stable propagation (A10÷A40). Table 2 shows the results. $J_{0,2\text{-}E}$ represents the value found in the intersection between J-curve ad the parallel line to Y axis drawn at 0.2 mm offset. $J_{0\text{-}N}$ denotes the J-value extrapolated to zero crack length. This approach has been considered as the experimental evidence shows a narrow and long crack (figure 4). Finally $J_{C\text{-}P}$ expresses the value found using the master curve method. In this method a double plot is performed in one diagram: load versus displacement, and crack growth versus displacement. When the crack growth curve separates from the X-axis, a perpendicular line to this axis is drawn. The J value is obtained from the intersection of the former line with the load-displacement register and the area enclosed within.

Fracture value results are displayed in figure 5. It can be appreciated that material

resistance to crack rises initially. Crazing extension and subsequent crack blunting will explain the toughness growth. At middle amount of glass beads (A6-A15 samples), the maximum in matrix plastic deformation and in fracture parameters is reached. J_{IC} decreases with higher particle content, being attributed to void coalescence and to a larger number of inclusions that are ineffective as craze generation points.

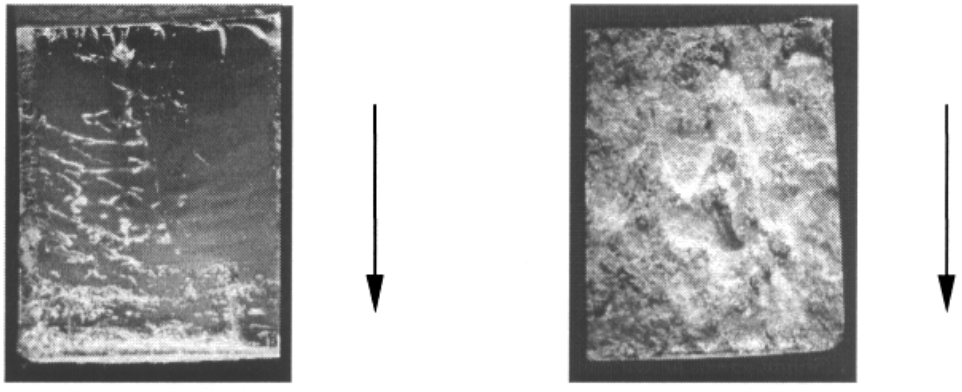

a b

Figure 6. Fracture surface roughness. Arrow indicates the propagating direction. a: PS, b: A15.

The examination of fracture surfaces by optical microscopy (figure 6-a) shows a mainly smooth appearance if glass content is null or very small (PS÷A2). For higher glass content, fracture surface becomes rough and irregular (figure 6–b). This change results from particle interaction with advancing crack front. In unfilled polystyrene, a craze could move forward in the matrix in a free way, however, in filled polystyrene a propagating crack is pinned at bead positions, to move ahead, crack has to round the inclusion. Once particle is surpassed, the crack-particle interaction is revealed by a set of steps that are located at particle front in the direction of crack front motion (figure 7). These steps are formed when crack front wraps around the particle on slightly different propagating planes as it breaks away [13].

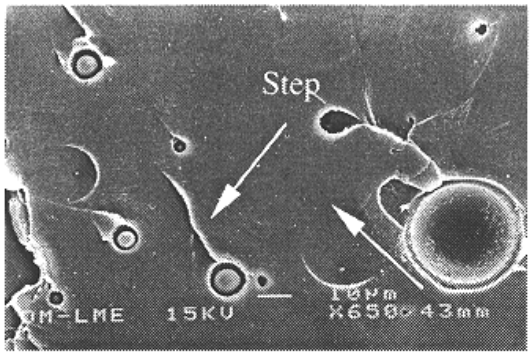

Figure 7. Fracture surface detail of A2 sample. Depicted zone is at the vicinity of notch. Arrow indicates the propagating direction

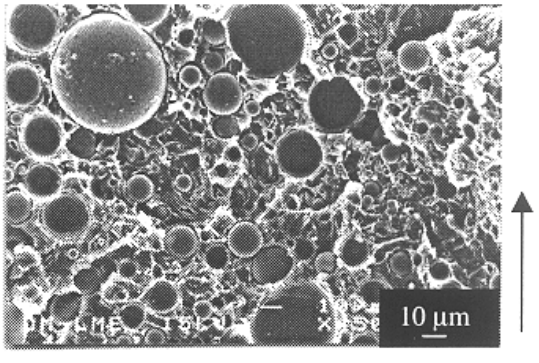

Figure 8. Scanning electron micrograph of central zone of A40 sample. Arrow indicates the propagating direction.

When samples are highly filled, interparticle distance is very small and the fracture path between a pair of particles is small too. As a result, high glass-filled polystyrene appears as a quasi-continuum medium for the propagating crack (Figure 8)

High strain rate

At high strain rates, samples fracture behaviour was always fragile and it has been analyzed entirely by LEFM criterion, nevertheless, progressive fracture stabilization was observed in the most filled composites. Table 3 summarizes K_{IC} and G_{IC} under impact conditions.

Table 3. Fracture parameters of polystyrene-glass bead composites at impact test velocity. (v=0.5 m/s).

Sample	K_{IC} (MPa. $m^{1/2}$)	r^2	G_{IC} (KJ/m^2)	r^2
PS	1.93	0.93	1.24	0.83
A2	2.07	0.93	1.36	0.76
A6	2.04	0.95	1.37	0.92
A10	2.01	0.97	1.30	0.90
A15	2.01	0.96	1.26	0.85
A25	1.85	0.97	1.03	0.89
A40	1.72	0.98	0.81	0.94

K_{IC} has an almost constant value of 2 MPa.$m^{1/2}$, decreasing in A25 and A40 blends. In impact conditions similar quantity of crazes are generated independently of the quantity of spheres added, it means that a small number of beads are enough to generate the maximum crazing in the matrix. Regarding with matrix interaction, particles are less effective at high strain rate than at low strain rate, as can be shown when comparing figures 6 and 9.

It can be observed that in impact K_{IC} is greater than at low rate testing. This could be explained by a warm up generated at the crack tip which tends to blunt the crack and inhibits crazing, both factors draw upon toughness rise. The evolution of G_{IC} with filler content varies in similar way with regard to the showed at low strain rate, however, relative increments between compositions are lower at high speed. This could be justified by the decrease in roughness found at high rates.

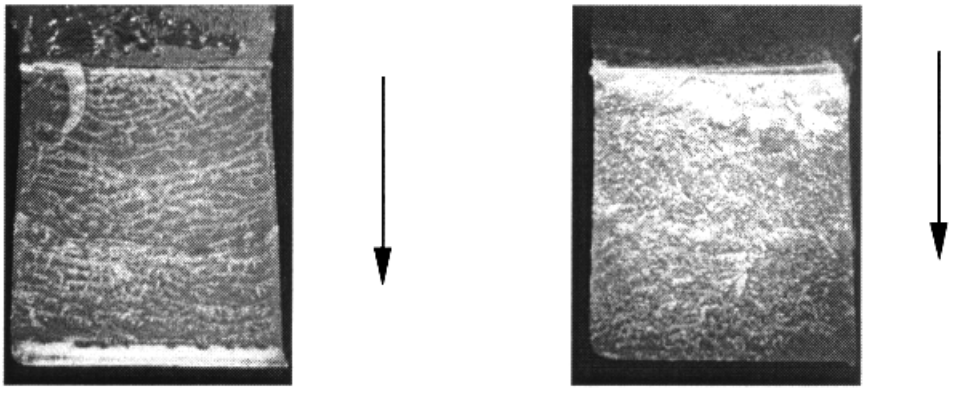

Figure 9. Fracture surface roughness, v=0.5 m/s. Arrow indicates the propagation direction. a: PS b: A15

Conclusions

The efficiency of the mixing process with a twin screw extruder has provided a good particle distribution in the matrix. On the other hand, the employment of a low viscosity matrix joined with small particles tends to diminish the phase segregation. Both factors have provided a set of composites formed by a polystyrene matrix filled with random dispersed inclusions.

Small quantities of glass beads are enough to modify polystyrene fracture behaviour changing the propagation mode, which tends to stabilize as more quantity of beds are added to matrix. There are not differences in the material resistance to crack between the initiation and the propagation stage.

Fracture parameters reach its maximum at moderate particle content, between 6 % wt and 15 % wt. Fracture energy increases due to fracture roughness increment, to crack-particle interaction, to fracture surface creation, and specially by the promotion of multiple crazing. Both low and high strain rates shows similar tendencies with regard to K_{IC} and G_{IC}, however, relative increments between compositions have been found to be lesser in impact conditions.

References

1. Kinloch AJ, Young RJ, (1983) Fracture Behaviour of Polymers. Chapman & Hall. London
2. Hertzberg RW. (1989) Deformation and Fracture Mechanics of Engineering Materials 3rd ed. John Wiley & Sons. New York
3. European Group of Fracture (1990) A Linear Elastic Fracture Mechanics (LEFM) Standard for Determining Kc and Gc for Plastics.
4. Moore DR, Pavan A, Williams JG, editors, (2001). Fracture Mechanics Testing Methods for Polymers Adhesives and Composites. ESIS Publication 28, Elsevier Sciencie Ltd. Oxford.
5. Narisawa I. Takemori MT (1989) Fracture Toughness of Impact Modified Polymers based on the J-Integral Polymer Engineering and Science Vol 29 num. 10 pp 671-678
6. Martínez AB, Maspoch MLL, (1994) Análisis de la Fractura y de la Deformación Plástica de Mezclas Multifásicas de Polímeros. Anales de Mecánica de la Fractura Vol 11 pp. 297-302.
7. Gupta RK (1994) Flow and Rheology in Polymers Composites Manufacturing.Ed. S.G. Advani, Elsevier Publishers, Amsterdam
8. Maspoch MLL, Martínez AB. (1990).Determinación de los parámetros de fractura del PS mediante el protocolo del E.G.F Anales de Mecánica de la Fractura, Vol 7, pp. 156-161
9. Sánchez-Soto M,(2000) Comportamiento Mecánico y Fractura de Mezclas de Poliestireno y Microesferas de Vidrio. Doctoral Thesis. Universitat Politécnica de Catalunya.
10. ASTM D-647.(1969) Rec. Practice of Design of Molds for Test Specimens of Plastics Molding Materials. American Society for Testing and Materials. Philadelphia. USA.
11. Ogadhoh SO, Papathanasiou TD. (1996) Particle Rearrangement of Glass–Reinforced Polystyrene by Injection Moulding. Composites A, Vol. 27
12. Dekkers MEJ. Heikens D. (1985) Stress Analysis near the tip of a Curvilinear Interfacial Crack between a rigid Spherical Inclusion and a Polymer Matrix. Journal of Materials Sciencie, Vol 20, pp 3865-3872.
13. Lange FF (1975) Fracture of Brittle Matrix, Particulate Composites in Mechanics of Composite Materials. Ed Robert M. Jones. Washington Scripta Books & co.